



An Assistant System For Blind To Avoid Obstacles Using Artificial Intelligence Techniques

Almajdoub, R.

Sebha University – Libya
Reim Almajdoub@fsc.Sebhau.edu.ly

Shiba, O.

Sebha University – Libya
Oma.Shibu@Sebhau.edu.ly

Abstract: This study focuses on developing an assistive system for blind individuals for collision avoidance of obstacles by combining artificial intelligence techniques; Convolutional Neural Networks (CNN), fuzzy logic control (FLC), and genetic algorithms (GA). This integrated system, named the (NFG) Neural Fuzzy Genetic). The proposed system combines artificial intelligence techniques through detecting and tracking objects, measuring the distance between objects and the blind person, and providing movement guidance using three ultrasonic sensors with FLC and optimization GA. The integration of these technologies offers an innovative solution to enhance the mobility and safety of blind individuals.

Specifically, object detection and tracking are applied through CNN, with an obstacle detection range of up to 40 meters. The obstacle recognition system is trained on the ResNet50 model, which includes 50 million trained images and more than 1,000 obstacle classifications, resulting in high accuracy in identifying and detecting obstacles. When tested, the accuracy of the trainer model reached 99.9%. FLC is then used to provide motor guidance and help make appropriate decisions in the presence of obstacles, navigate safely and independently, and determine movement directions in obstacle-free paths with the help of three sensors. The person moves at a steering angle determined by fuzzy rules. Information from Ultrasonic is the input for FLC, and GA was used to automatically generate the fuzzy rules base and membership functions to optimize the performance of the FLC, experimental results conducted for collision avoidance simulation also showed that the proposed system is capable of avoiding collisions of obstacles and the blind assistive.

IndexTerms --- Object detection, Smart Glasses, Smart Stick, Blind individuals, Convolutional Neural Networks (CNN), Fuzzy Logic Control (FLC), Genetic Algorithm (GA), Visual Impairment, Avoid Collision.

I. INTRODUCTION

The World Health Organization (WHO) reported that; “Vision impairment and blind impact the life of people everywhere. In low- and middle-income settings the burden of vision impairment can be even greater due to fewer opportunities to access the most essential eye

care services”, “Ref. [1]”. According to “Ref. [2]”. “Cataracts and uncorrected refractive errors are estimated to be the leading causes of blind; however, other causes for blind cannot be ignored. Age-related macular degeneration, glaucoma, long-standing systemic conditions like diabetes causing diabetic retinopathy, infectious diseases of the eye, and trauma to the eye are all equally important causes for vision impairment that need to be addressed”. Safe and independent mobility is considered one of the difficult problems facing blind persons in their lives, due to the diversity of the surrounding world, as vision impairment and blindness people worldwide face daily many challenges and dangers while their natural activities and work, especially in the unknown environments. Therefore, we have searched for solutions to support and assist blind communities. As a result of our search, we found that the vision impairment and blind communities’ needs for support, assistance orientation, and mobile devices have increased according to the frightening increase in the number of vision impairment and blind people as well as the lasted development of the technologies in all fields of the human’s life. Although many kinds of devices and glasses are available for blind persons worldwide, those devices and glasses cannot provide vision impairment and blind communities with all the information and features for safe mobility, that are available to people with sight “Ref. [3]”. as people with visual impairments have many difficulties carrying out daily tasks, like safely traveling and identifying objects, especially in unfamiliar places, these duties can be very hazardous and challenging “Ref. [4]”.

systems that utilize RGB-D (Red, Green, Blue, and Depth) sensors “Ref. [5][6]”, as opposed to other sensor-based certain for obstacle avoidance to get over these restrictions. This paper suggests a multi-sensor fusion a technique that combines ultrasonic and depth sensors. Sensors that are tactile or aural can provide information to those who are blind “Ref. [7]”. An essential source of sensory input, auditory perception, is not hindered by tactile feedback. Nevertheless, tactile techniques are inappropriate for wearable ETA

Received 13 Apr , 2024; revised 04 May, 2024; accepted 15 Mar 2024. Available online 08 Aug, 2024

devices (like the glasses suggested in this work) due to their huge size and significant power consumption. As a result, in some situations, sound or artificial voice is a possibility. To aid blind people in seeing their environment, several sound feedback-based ETAs translate processed RGB or depth images into acoustic patterns “Ref. [8]”, or semantic speech “Ref. [9]”. To make decisions, the blind individual must still comprehend and interpret the feedback sound. As a result, these systems find it difficult to guarantee that blind people make wise judgments based on reliable feedback. To solve this problem, this study creates three different audio cues that direct users in the right route. These cues are generated from the traversable direction identified by the multi-sensor fusion-based obstacle avoidance algorithm. compared to other senses like touch and hearing, vision offers more information, therefore people with impaired vision can benefit from visual perception. Moreover, these devices don't provide a complete solution that can assist communities with vision impairment and blindness in all aspects of their lives. one of the most important reasons for delving into this study is to design an effective system that helps blind people by providing movement directions to avoid collisions with obstacles. This is done by combining the advantages of the three smart logic systems and integrating them into one system, which is the proposed system NFG, and achieve a high accuracy range for obstacle detection, and tracking moving obstacles, in known and unknown environments, the organization of this paper is the following: The relevant literature on guiding individuals with blind is reviewed in Section II. In Section III, the proposed smart system is shown. The efficacy and resilience of the system are illustrated by the experimental findings presented in Section IV, and the proposed study versus related study in Section V, the conclusion, and the recommendations are in Section VI.

II. RELATED WORKS

There are many problems facing scientists in the phenomenon of obstacle avoidance for the blind and finding appropriate methods that rely on artificial intelligence and deep learning algorithms. Also, presenting ways to find solutions for individuals with visual impairment in the scientific field is a source of challenge for scientists, in this section, the relevant literature on obstacle avoidance and guidance feedback is reviewed.

A. Obstacle Avoidance

The identification and avoidance of obstacles has been the subject of extensive investigation. Obstacle avoidance techniques can be divided into three categories based on the kind of sensors used: ultrasonic sensor-based “Ref. [12]”, laser scanner-based “Ref. [13]”, and camera-based “Ref. [14]”. Approaches using ultrasonic sensors gauge the distance to impediments and compare the result to a preset threshold to decide when to move forward. They may experience signal problems or interference in inside areas, particularly when utilizing ultrasonic radar or sensor arrays, and they do not offer exact directional information. Still,

they work in dark conditions and detect obstacles close to the person. Because laser scanners have such great resolution and precision, they are frequently used in mobile robot navigation. Unfortunately, their high cost, weight, and power consumption render them unsuitable for wearable navigation systems.

RGB-D cameras are popular because of their low cost, small size, and ability to deliver detailed information. They combine dense range information from active sensing with color information from passive sensors, such as conventional cameras. One RGB-D camera-based solution uses both range and color information to extend floor segmentation and detect detailed obstacles. Another approach generates a 3D voxel representation of the environment and evaluates 3D Travers's ability for obstacle avoidance. However, due to depth camera restrictions, these solutions are only applicable to cases involving non-transparent objects.

B. Guiding Information Feedback

There are three main approaches for delivering advice to vision-impaired people: haptic, auditory, and visual. Vibrators are commonly used in haptic feedback systems on belts “Ref. [17]”, helmets “Ref. [18]”, and backpacks “Ref. [19]”. While they have low interference with environmental sensing, they struggle to relay complicated information and require substantial training and focus. Audio feedback systems make use of acoustic patterns, semantic speech, variable sound intensities, or spatially targeted auditory cues. In “Ref. [20]”, the processed RGB image is directly translated to audio patterns, allowing blind people to perceive their environment, the depth image is transformed into semantic speech to convey information about obstructions. In “Ref. [21]”, the depth image is converted to various sound intensities to represent barriers at varied distances., the depth image is translated into spatially specific aural cues to convey 3D information about the environment. However, these audio cues can be misinterpreted in busy or complex situations.

Visual feedback systems are ideal for people with impaired sight because they provide more comprehensive information than haptic or acoustic feedback systems, the distance of an obstacle is mapped to brightness on an LED (Light Emitting Diode) display as a visual augmentation tool to assist users in detecting obstacles. However, the LED display's low resolution restricts its capacity to display minor impediments “Ref. [22]”, this solution does not represent an appropriate solution that can help the blind in all aspects of their lives. and therefore; This study proposes a new system that integrates both artificial intelligence technologies to provide the appropriate solution for blind individuals and lead their normal lives. to address these shortcomings, this work presents a unique obstacle avoidance algorithm based on multi-sensor fusion. This method uses depth and ultrasonic sensors to calculate the most traversable path. The output traversable direction is then transformed into three forms of aural cues, allowing the user to choose the most appropriate cue in various settings. These aural signals are combined with an augmented reality

(AR)--based visual enhancement system to assist blind individuals.

III. THE PROPOSED SYSTEM

The proposed system was based on combining some of the advantages of the three intelligent logic systems. This intelligent system combines in a very simple way the imitation of some functions logic of the human brain (provided by a CNN) and reliability simulation and discrimination to several different levels of any variable during decision making (provided by FLC) then combines it with powerful and evolutionary search methods that can search for structures in addition to numerical parameters (provided by GA), these technologies offer an innovative solution to enhance the mobility and safety of blind individuals. The proposed system relies on the presence of a camera mounted on glasses, and a headset connected to these glasses, the camera's role is to capture high-resolution videos and still images. the camera output is then sent to the control module for further analysis. to perform image recognition, we require a dataset along with corresponding labels that describe the contents of the images. and the presence of three ultrasonic motion sensors mounted on a stick at three angles: 45, 90, and 135 to detect obstacles and determine the angle at which the obstacle is located, especially obstacles that are difficult to identify through the camera or if the situation is Because visibility is poor at night, the best course of action is determined, where connected three sensors, and a breadboard, an Arduino Uno board, and wires, are placed in a box attached to a stick.

A CNN deep learning model is an alternative to the camera mounted on the glasses to identify and detect obstacles, Similar individuals and cars are identified as obstacles in the roadway, and the range of obstacle detection using computer vision techniques is up to 40 meters, as well the distance measurement using three sensors that movement guide with a range of 4 meters to 6 meters and are inputs for FLC, FLC is then used to provide motor guidance and help make appropriate decisions in the presence of obstacles, navigate safely and independently, and determine movement directions in obstacle-free paths with the help of three sensors. The person moves at a steering angle determined by fuzzy rules. and GA was used to automatically generate the fuzzy rules base and membership functions to optimize the performance of the FLC. This hybrid system updates the cognitive foundations of the words for the controller face to decide the route that blind individuals need to travel. To allow him to cross the street in three steps, he wears glasses and wears a headset that is placed on his ear. The headset interprets his movements, whether they are forward, right, left, or stopped. the ResNet50 model is used to train the obstacle detection system, along with 50 million trained photos and more, with 1,000 obstacle classes and high obstacle identification accuracy, this proposed system algorithm combining artificial intelligence techniques shown in Figure 1, provides speed for obstacle detection, obstacle avoidance, and guidance/arrival at the desired location.

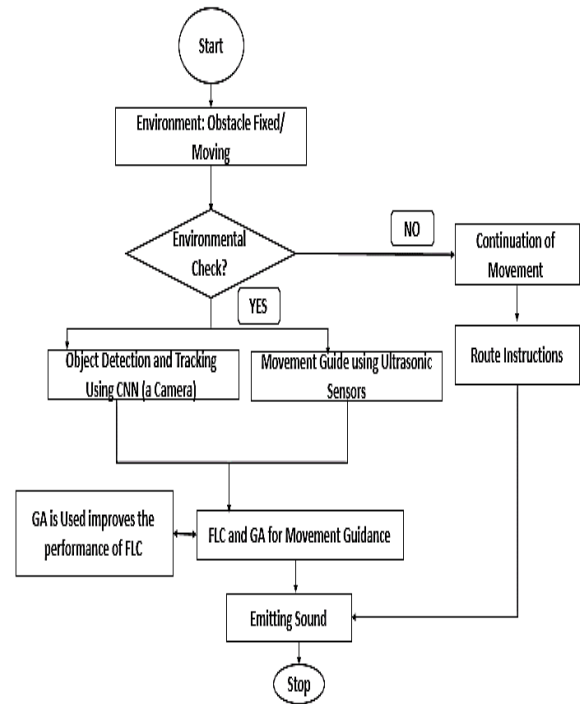


Figure 1: Flowchart of the Complete Proposed System Algorithm Combining Artificial Intelligence Techniques.

A. Structure and Hardware Components for Proposed System

This section gives a summary of the structure and hardware of the proposed system.

• Smart Glasses System for Blind Individuals

Recognizing the faces and identifying information of friends and family members is one of the most crucial and critical jobs for blind individuals. A face recognition system was developed by Daescu et al. "Ref. [23]"; that can process facial photos taken with a Smart Glasses camera in response to user inputs, process the results on a server, and then provide an audible response. A pair of cellphones, smart glasses, and a back-end server are used in the client-server architecture of the system to do face recognition utilizing deep CNN models like FaceNet and Inception-ResNet50. It will take longer for this face recognition system to operate since it must be retrained to identify new faces that are not stored on the server. Mandal and associates "Ref. [24]". centered on the capacity to identify faces across a range of lighting scenarios and facial expressions. To accomplish within-subclass discriminant analysis, a wearable face recognition system built on Google Glasses was created. Nevertheless, this approach had a well-known issue: even though it identified the faces of 10 subjects accurately, the model needed to be retrained for additional faces that weren't included in the original dataset.

Architecture of the proposed system which is comprised of a portable computational hardware module and a CNN model. The hardware components consist of a camera and a neural network using a computer system; the camera takes digital images, which are then sent to the computer system for additional processing. Figure 2 shows how the system is assembled and designed using SolidWorks for the proposed system.



Figure 2: Smart Glasses Model for the Proposed System.

The CNN method is the main strategy used in this study. for obstacle detection and tracking, and the user is guided by the audio speaker output. Figure 3 shows The hardware components we need to design the proposed system.

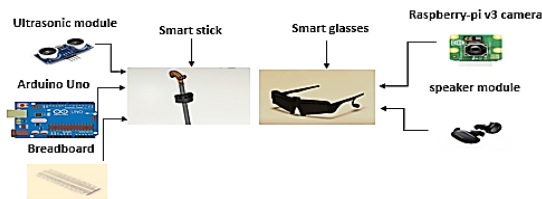


Figure 3: Hardware Components for Design of the Proposed System.

• *Smart Stick for Blind Individuals*

One of the main concerns for blind individuals is obstacle detection. This project presents a Smart Stick of blind that uses an Arduino UNO and ultrasonic sensors. The main objective of this project is to help blind individuals walk more easily and to warn them whenever an object or person blocks their path. To do this, a voice module is connected to the circuit and emits a warning voice that indicates the direction of the object—for example, if it is on the left, it will say "Careful Object in Left"—as well as three ultrasonic sensors connected to the left, right, and center to measure the distance from any obstacles. and a 5V battery to run the apparatus, the components have been connected as in “Ref. [25]”. Below is the full Smart Stick for the blind circuit schematic for the proposed system shown in Figure 4. Since we just need to connect one JQ6500 voice module and three ultrasonic sensors, it is rather easy to do.

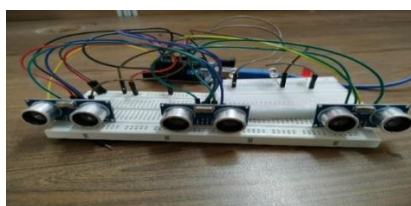


Figure 4: Hardware Components for Smart Stick for Blind Individuals for the Proposed System.

Nine-volt batteries are used to power the entire board. Arduino UNO is the circuit's brains. The left, right, and front of the stick each have three ultrasonic sensors that are used to identify obstacles. VCC and GND, two of the four pins of these three sensors, are linked to the GND and 5V of the Arduino. Since the JQ5600 MP3 module operates on 3.3V logic, it cannot be directly connected

to the Arduino's IO pins. However, it can be powered via the Arduino's 5V power line. The digital pins 9 and 8 of the Arduino UNO are linked to the RX and TX pins of the MP3 module. To reduce the voltage of the Arduino, a 1kΩ resistor is placed between the digital pin 9 of the Arduino UNO and the MP3 module RX “Ref. [25]”. Figure 5 illustrates where the sensors are located; each sensor is positioned at a different angle to maximize coverage of the area in front of it and enable various obstacle detection techniques. 3.5 meters is the greatest detecting range; yet, the ultrasonic sensor's maximum permitted range is from 4 m to 6m. Since only these obstacles need to be avoided by the user, overhead impediments are recognized up to 1.2 meters in the air.



Figure 5: Smart Stick with Three Ultrasonic Sensors for the Proposed System.

The final system, which combines Smart Glasses and a Smart Stick for object detection and tracking, uses a camera to detect objects and measure the distance between a blind person and them. It then uses algorithms to detect the distance and three ultrasonic sensors fixed on the Smart Stick to measure the distance to nearby objects. In the dark and at night, the three ultrasonic sensors on the Smart Stick blind can also measure the distance. The system then sends the appropriate decision to the speaker to guide the blind individuals in the correct direction. Figure 6 illustrates the model design for our system using SolidWorks programs.



Figure 6: Final Model Design for the Proposed Smart System Combination of Smart Glasses and Smart Stick.

B. Software Methodology for Proposed System

For the software aspect, the proposed system was built on MATLAB R2022b with MATLAB/Simulink simulation, especially since it is necessary to build the system on a copy of MATLAB is modern, and this is one of the most important requirements for the proposed system, and it was implemented as follows:

• *Objects Detection and Tracking Using CNN*

To identify items in the blind person's surroundings, the system makes use of an object detection and tracking algorithm based on neural network technology. The CNN model can reliably detect and classify objects because it was trained on a large dataset of annotated images. The CNN's output tells us which objects are around the blind individual, where, and what kind of objects they are. A substantial dataset of 50 million photos, including 1,000 obstacle classifications, is used to train the CNN deep learning model. The system can accurately recognize obstacles due to this thorough training, which guarantees quick and dependable obstacle recognition.

CNNs are types of Artificial Neural Network models that replicate the visual cortex, which is a fully connected network comprising layers that are sensitive to specific visual fields. These networks are made especially to use spatially connected data efficiently. Convolutional, activation, pooling, and fully connected layers make up the tiered structure of CNNs, with at least one convolutional layer per network "Ref. [26]". The convolutional layer, which is made up of neurons grouped in three dimensions—the width, height, and depth of the activation volume—takes use of the spatial relationship in the input data. This layer produces an activation map or feature map mathematically by computing the dot product between the weights of the connected region in the input volume and the local receptive fields in the input. In the layer below, every local receptive field is linked to a hidden neuron. However, because the convolutional layer transforms the input linearly, it isn't satisfied with the universal approximation theorem "Ref. [27] [28]", implying that linearity restricts the network's capacity for representation. An activation layer is added to the network to introduce non-linearities to address this. To make the feature map created by earlier layers simpler, the output of this layer is then down-sampled or pooled in the pooling layer. The pooling layer takes advantage of the notion that a feature's relative position to other identified features matters more than its exact location within the feature map. This lowers the representation's spatial size, which lowers computing expenses and lessens the effects of overfitting. Subsequently, the complete stack is combined into a fully linked layer, in which every neuron in the layer above is coupled to every other neuron. Usually one-dimensional, the fully connected layer indicates the labels for classification. It produces a score for each classification label.

Because CNNs can make use of the spatial relations between items in the given data, they perform very well in tasks that entail manipulating geographically connected data, including object detection or recognition. Additionally, CNNs offer a simplified method for encoding data and creating networks with a great deal fewer parameters because they operate under the assumption that the inputs are images. While humans can quickly recognize and categorize visual data, machines find image classification to be a challenging undertaking. There are several steps involved in image classification, such as acquiring the image, pre-processing it, detecting it, extracting features, and

classifying it. CNN baseline architecture is shown in "Ref. [30]", the primary components of the data are identified by transforming, denoising, and analyzing the images during pre-processing. Subsequently, these photos undergo detection and feature extraction procedures to pinpoint important things. To identify important items, the retrieved attributes are subsequently subjected to detection and feature extraction procedures. The objects are categorized into predefined classes in the image database using the extracted features, "Ref. [31] [32]".

By adding more layers to improve the quality of the characteristics in the data, a deep network is essential to get better results than other networks. To create an object identification system that helps visually challenged people, this research paper focuses on real-time image classification in a three-dimensional space utilizing a Deep CNNs "Ref. [29]". and the AlexNet dataset, uses the ResNet50 network model dataset for object identification for visually challenged individuals, and pre-trained using YOLO v3 algorithm, was used and added to our model, adjusting the resolution to scaling 416 x 416 to preserve and reduce information while lowering the computational load, and the frame rate for camera stream is 30Fps. the training using Faster R-CNN for detection and classification with new images dataset that was added to increase the accuracy of the model. it was found that the accuracy reached 99.9% for identifying obstacles, the crosswalk signals were identified as "safe-to-cross" or "do-not-cross" using a cascade classifier that set an area of interest (Region of Interest ROI) based on LBP features "Ref. [31]". Real-time performance and excellent accuracy were prerequisites for both ROI identification and This was crucial since a user may proceed through a "do-not-cross" indication if they were misclassified. Moreover, real-time performance was required since delays could cause the "safe-to-cross" sign to go unnoticed. Shown block schematic in "Ref. [31]" the system's whole pipeline, the input frame from the smart glasses served as the new frame, and every module operated based on its present condition.

ROI classification; basic CNNs were employed. Four blocks make up the network's structure: a max-pooling layer, two convolution layers, and one. After each convolution layer, a dropout layer was added, and after each max pooling layer, a batch normalization layer. was added. Two completely connected layers were used to categorize the inputs. Three distinct classes—"background," "safe-to-cross," and "do-not cross"—were employed, applying VGG16 parameters for transfer learning "Ref. [30]". Any input labeled as "background" was not to be confused with "do not cross" or "safe to cross." Since our target images had few features and the network was prone to overfitting, the background training data prevented overfitting. There are more advanced CNNs available (Yolov3), There were two steps involved in updating the user position:

prediction and correction. In the Kalman Filter's prediction step, pre-integration fusion was used, The Kalman filter's correction step used the results of solving the perspective-n-point problem with matching

3D virtual coordinates of the detected crosswalk sign and 2D image pixel points, Kalman filters are used to track objects by color contrast. Throughout the entire network, a variety of activation functions, including ReLU and Exponential Linear Units (ELU), are employed. These functions serve to bring the average activation closer to zero, thereby accelerating the learning speed. The ELU can be defined through the following "Equation (1)":

$$f(x) = \begin{cases} x & \text{if } x \geq 0 \\ a[\exp(x) - 1] & \text{otherwise} \end{cases} \quad (1)$$

Where a is the hyper-parameter that is set and $a \geq 0$, "Ref. [30]".

• **Distance Measurement Using Computer Vision Techniques**

Use the proposed study to measure the distance between the person and detected objects through computer vision techniques by utilizing depth estimation algorithms and stereo vision techniques, the system can calculate the distance to objects based on their perceived size and position in the image, this distance information is crucial for determining the proximity of objects and assessing potential collision risks "Ref. [32][33]", this was calculated through the following "Equation (2)" "Ref.[34]":

$$\text{Distance (m)} = \frac{(2 \times 3.14 \times 180)}{(w + h \times 360) \times 1000 + 25} \quad (2)$$

Where w : width, h : height, the number 25 represents the pixel size, through these equations and Using this approach to measuring distance, the proposed study was able to detect obstacles to a range of 40 meters.

• **Movement Guide using Ultrasonic Sensors**

Three ultrasonic sensors are used to offer movement direction. These sensors detect the amount of time it takes for ultrasonic waves to return after colliding with an item. The system can identify obstacles in the blind person's path and provide the necessary movement instructions by evaluating the sensor data. The user can reliably identify obstacles that are close to them with the help of ultrasonic sensors. This smart stick's primary function is obstacle detection, which is accomplished via ultrasonic sensors. An ultrasonic sensor uses high-frequency vibrations to identify every object that gets in the user's path. The object reflects the ultrasonic waves, allowing the ultrasonic sensor to detect them. The distance between the sensor and the object can be determined by timing the interval between sending and receiving sound waves "Ref. [35] [36] [37]", the distance is calculated from the following "Equation (3)" "Ref. [35]":

$$\text{Distance (cm)} = \frac{\text{Speed of sound (cm/}\mu\text{s)} \times \text{Time}(\mu\text{s})}{2} \quad (3)$$

The three ultrasonic motion sensors precisely detect the angle at which an impediment is located. They are angled at 45, 90, and 135 degrees. The system can accurately locate barriers and guide a person based on

this information when combined with distance measurement.

• **Approach Obstacle Collision Avoidance**

A robot will be simulated in a MATLAB/Simulink environment using ultrasonic sensors to test the proposed obstacle collision avoidance algorithm and motion path planning in a virtual environment. To simulate a person in a MATLAB/Simulink environment, we need to add some other sensors, such as motion sensors, speed sensors, and positioning sensors, such as GPS. The simulation has been implemented using the force vector method as in "Ref. [47] [49]". The tricycle is the type of mobile robot employed in this work; it features two independent aft wheels and a wheel in front to provide stability while being displaced. The mobile robot's primary task is to determine the distance and target-robot angle to arrive at the arrival configuration known as the target. The specifications of the mobile robot that was used are shown in Figure 7.

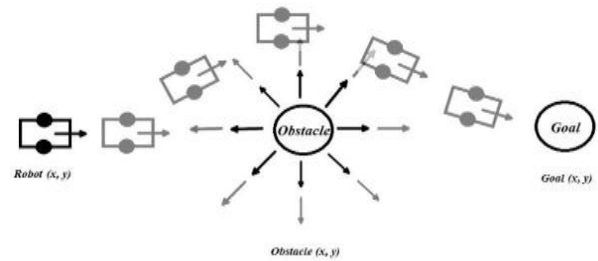


Figure 7: Robot moving toward a target and avoiding the obstacle "Ref. [47]".

The movement of the blind person is analyzed, and his movement is explained on the robot in Figure 8. This is done by calculating the angle between the robot and the target, then calculating the angle between the robot and the obstacle, and calculating the variables that affect the speed until control is created through which the robot moves in the correct path to avoid the obstacle and reach it. to the target at the shortest distance and in the shortest time.

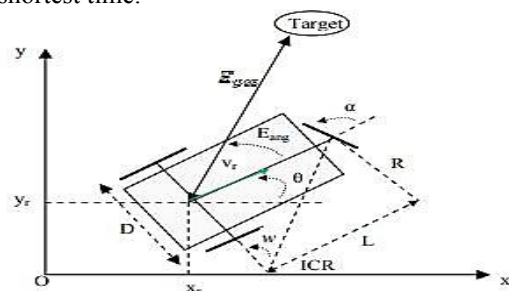


Figure 8: Tricycle mobile robot "Ref. [48]".

For the simulation, the kinematic model is used in "Equation (4)" following:

$$\begin{cases} \dot{x} = v_r \cos(\theta) \\ \dot{y} = v_r \sin(\theta) \\ \dot{\theta} = \frac{v_r}{L} \text{tg}(\alpha) \end{cases} \quad (4)$$

whose discrete form is given by "Equation (5)":

$$\begin{cases} x(k+1) = x(k) + \Delta t \cdot v_r(k) \cdot \cos(\theta(k)) \\ y(k+1) = y(k) + \Delta t \cdot v_r(k) \cdot \sin(\theta(k)) \\ \theta(k+1) = \theta(k) + \Delta t \cdot \frac{v_r(k)}{L} \text{tg}(\alpha(k)) \end{cases} \quad (5)$$

α : Steering angle.

v_r : Navigation speed of the robot.

θ : Robot orientation.

w : Revolution speed of the robot around its instantaneous CIR.

Epos: Distance between the robot and the target.

Eang: Angle between the current robot orientation and that of the target.

L : Frame length.

D : Robot width. x_r, y_r : Robot coordinates.

A unit force vector (\vec{F}_t) that is directed from the robot to the target location serves as the representation of the target. A unit force vector (\vec{F}_o) pointing in the direction of the robot from the nearest obstacle location indicates the obstacle avoidance direction "Ref. [49]", Figure 9 shows the analysis of two forces and theta and alpha.

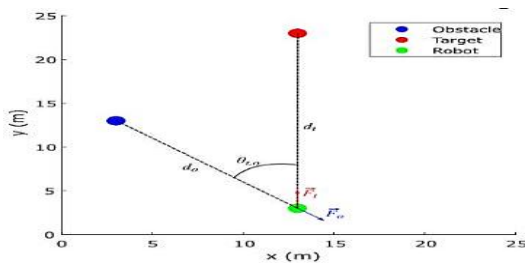


Figure 9: Analysis of the Movement "Ref. [49]".

collision-free direction for the robot is given by "Equation (6)":

$$\vec{F} = w\vec{F}_o + (1-w)\vec{F}_t, \text{ where } 0 \leq w \leq 1 \quad (6)$$

$$\theta = \angle \vec{F}$$

to $[-\frac{\pi}{4}, \frac{\pi}{4}]$. Therefore, if the current robot direction is $\theta_r(k)$, the next direction is calculated as:

$$\theta_r(k+1) = \theta_r(k) + \min\left(\max\left(\theta - \theta_r(k), \frac{\pi}{4}\right), -\frac{\pi}{4}\right) \quad (7)$$

The weight w of the force vector \vec{F}_o is calculated using function f_w :

$$w = f_w(\alpha, \theta_t) \quad (8)$$

Where:

- $a = \frac{d_o}{d_t}$ is the ratio of the robot-to-obstacle distance (d_o) and the robot-to-target-distance (d_t)
- $\theta_{t,o}$ is the absolute difference between the target and obstacle directions concerning the robot.

The function f_w must produce high w values, or concentrate on avoiding the obstacle, to complete the navigation task when:

- Both the target and obstacle directions from the robot are similar ($\theta_{L,o}$ is low)

- The obstacle is closer to the robot than the target (α is low).

Otherwise, f_w must generate low w values, that is, focus on reaching the target. Figure 10 shows the methodology

for path planning and simulation obstacle collision avoidance.

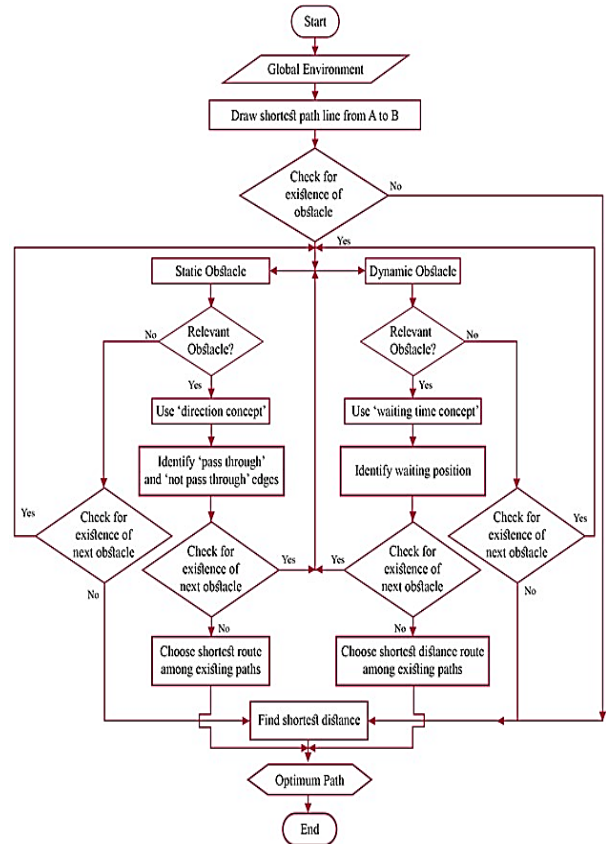


Figure 10: Flowchart of Steps in Path Planning of Obstacle Collision Avoidance "Ref. [50]".

a. FIS Initialization

The (Fuzzy Inference System FIS) is initialized using the mamfis function, which creates a Mamdani-Type FIS object. two input variables, alpha, and theta_t_o, are added to the FIS using the addInput function. The input ranges and names are specified as [0,2] and [0 pi/2] for alpha and theta_t_o, respectively for the first test with 3 Membership for each input.

▪ Fuzzification

Triangular fuzzy membership functions (triangular) are used for fuzzification, the triangular function takes the sensor value, defining the membership function shape.

▪ Membership Function Definition

Membership functions (MFs) are essential components of a Fuzzy Inference System FIS, as they define the fuzzy sets and their shapes. In this section, the MFs for each input and output variable are defined.

▪ Input Variable (Alpha)

Three MFs are defined for the alpha variable: 'low', 'Medium', and 'high'. The 'low' MF is a zero-order membership function (MF) with a range of [0, 0.5]. The 'Medium' MF is a triangular membership function

(trimf) with the points [0.5, 1, 1.5]. The 'high' MF is a first-order membership function (SMF) with a range of [1.5, 2].

- **Input Variable (θ_{t_o})**

Three MFs are defined for the θ_{t_o} variable: 'low', 'Medium', and 'high'. The 'low' MF is a zmf with a range of [0, $\pi/8$]. The 'Medium' MF is a trimf with the points [$\pi/8$, $\pi/6$, $\pi/4$]. The 'high' MF is an SMF with a range of [$\pi/4$, $\pi/2$].

- **Output Variable (Weight w)**

Three MFs are defined for the output variable w : 'low', 'Medium', and 'high'. The 'low' MF is a zmf with a range of [0, 0.25]. The 'Medium' MF is a trimf with the points [0.25, 0.5, 0.75]. The 'high' MF is an SMF with a range of [0.75, 1].

- **FIS Output Definition**

The output variable w is added to the FIS using the addOutput function. The output range is specified as [0,1], and the name is set as 'w'. This method is called force vectors in robot systems.

- **Defuzzification**

Defuzzification is performed using the center of gravity (COG) method. The weighted averages are divided by the sum of the rule-optimized values to normalize the results.

b. FLC and GA for Movement Guidance for Simulation Obstacle Collision Avoidance

Including an FLC in the GA can prevent precocity by dynamically generating the crossover rate (Pc) and mutation rate (Pm). The idea of combining an FLC and a GA is described in "Ref. [40]".

The GA portion provides the input parameters to the fuzzification interface at the start of each generation. The interface then converts the parameters into fuzzy state inputs and sends them to the FLC system, where the inference operation generates the fuzzy state output. Finally, the defuzzification interface's output parameter is taken into account as the input parameter for the current generation.

- **Genetic Operation**

In this proposed study, a set of fuzzy rules is represented by a binary string. Since the simulation system requires 8,16,32 fuzzy rules and each rule requires 3 bits, each binary string comprises 24, and 48,96 bits. The roulette wheel selection is used by the GA to carry out this task. "Equation (9)" defines the ratio that is selected from each individual in the population "Ref. [40]".

$$P(i) = \frac{\text{FitnessValue}(i)}{\sum_{j=1}^n \text{FitnessValue}(j)} \quad (9)$$

Define the two individuals P_i and P_j as:

$$P_i = x_{i,1}x_{i,2}x_{i,3} \dots x_{i,k-1}x_{i,k}x_{i,k+1} \dots x_{i,n} \quad (10)$$

$$P_j = x_{j,1}x_{j,2}x_{j,3} \dots x_{j,k-1}x_{j,k}x_{j,k+1} \dots x_{j,n} \quad (11)$$

If the crossover operator begins at the k th bit, then the new offspring chromosomes are:

$$C_i = x_{i,1}x_{i,2}x_{i,3} \dots x_{i,k-1}x_{j,k}x_{j,k+1} \dots x_{j,n} \quad (12)$$

$$C_j = x_{j,1}x_{j,2}x_{j,3} \dots x_{j,k-1}x_{i,k}x_{i,k+1} \dots x_{i,n} \quad (13)$$

If the mutation operator occurs in the k th bit of the individual P_i , then:

$$P_i = x_{i,1}x_{i,2}x_{i,3} \dots x_{i,k-1}\bar{x}_{i,k}x_{i,k+1} \dots x_{i,n} \quad (14)$$

- **Evaluation Function**

The equation represents a normalized evaluation function based on the control system's performance in "Equation (15)" "Ref. [40]":

$$\text{Fitness} = \alpha \frac{\sigma_m - \sigma_s}{\sigma_{sw}} + \beta \frac{t_{sm}^{-t_s}}{t_{sw}} + \gamma \frac{e_{sm} - e_x}{e_{sm}} \quad (15)$$

where σ , t_s , e_s are the overshoot, rise time, and steady-state error of the control system respectively, σ_m , t_{sm} , e_{sm} are the maximal values of the overshoot, rise time, and steady-state error "Ref. [40]".

$$H(s) = \frac{20e^{0.02s}}{1.6s^2 + 4.4s + 1} \quad (16)$$

The simulation is implemented using MATLAB R2022b, Using the fuzzy rules that are optimized by automatically generated using GA and is optimized through the configuration of the genetic algorithm's optimization parameters. The population size is limited to 200 to increase the likelihood of discovering better solutions. The maximum number of generations is 50, though this can be changed if more parameter adjustment is needed.

IV. EXPERIMENT AND ANALYZE THE RESULTS

The next step is to experiment and the proposed system test(NFG). This system's main goal is to detect objects and pinpoint their locations, track moving obstacles, measure the distance between a person and an obstacle (up to 40 m), and movement guidance using FLC with GA. and tested the system on five recorded videos, the user can provide voice instructions when they are looking for something or need help finding it, it recognizes their voice input and uses the audio speaker output to guide them to the desired destination, in terms of spotting obstructions, averting crashes, and directing the user to their intended location, the suggested system exhibits amazing speed and precision. The system's efficacy and dependability have been confirmed after extensive testing and evaluation. this is turned out through experiment and testing, Figure 11 shows the result of object detection in recorded video using the CNN model, which achieved an accuracy rate of up to 99.9% when tested to detect objects, where the obstacle is detected by placing a rectangle on the detected obstacle, where the screen is divided into two axes (X, Y) to determine the location of the detected obstacle, whether on the right the left, or in the middle, Then Motion

Guidance by FLC and GA through information received from Ultrasonic sensors through voice instructions that appear on the comments window in MATLAB.

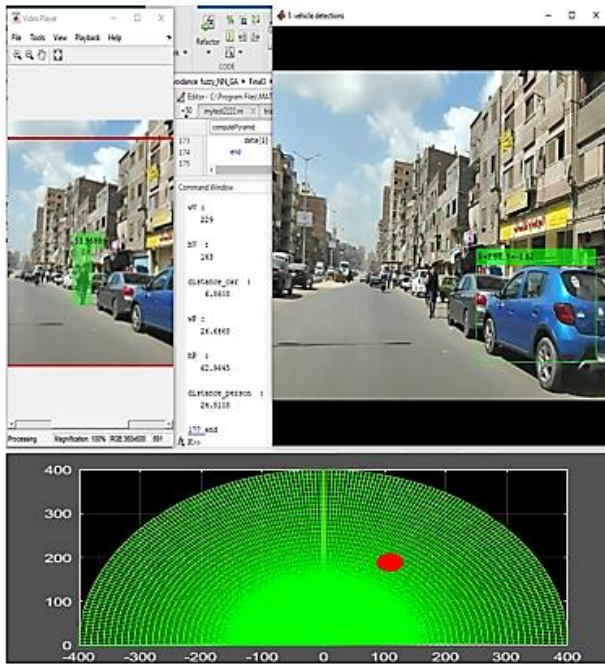


Figure 11: Result Detection Object in the Recorded Video by CNN and Motion Guidance by FLC and GA.

Three experiments were conducted to test the FLC with GA to test the number of rules that would be created based on the number of inputs and the number of membership functions. In the first experiment, three membership functions with two inputs were used. In the second experiment, four membership functions with two inputs were used. The three experiments used six membership functions with two inputs, this is to test the accuracy of reaching the target with the smallest angle, the minimum distance, the minimum time, and the minimum deviation from the obstacle.

A. Test 1 (FLC+GA+2 Inputs and 3 MS)

In the first experiment, in Table 1 there are two inputs: alpha and theta. with three memberships function, and in Table 2 one output: weight with three memberships function.

Table 1: Membership Functions for Input Variables

Variable	Membership Function	Parameters
alpha	low	[0, 0.5]
alpha	Medium	[0.5, 1, 1.5]
alpha	high	[1.5, 2]
theta_t_o	low	[0, pi/8]
theta_t_o	Medium	[pi/8, pi/6, pi/4]
theta_t_o	high	[pi/4, pi/2]

Table 2: Membership Functions for Output Variable

Variable	Membership Function	Parameters
w	low	[0, 0.25]
w	Medium	[0.25, 0.5, 0.75]
w	high	[0.75, 1]

We see in Figure 12 shown below A, B, and C the results of the first experiment, where the number of 8 rules were created after removing the unimportant rules that affect the accuracy of the robot's movement after evaluating the result. We also notice the effect of the GA on the creation of fuzzy rules. Show Figure 13,14 to create rules and angles for the first experiment.

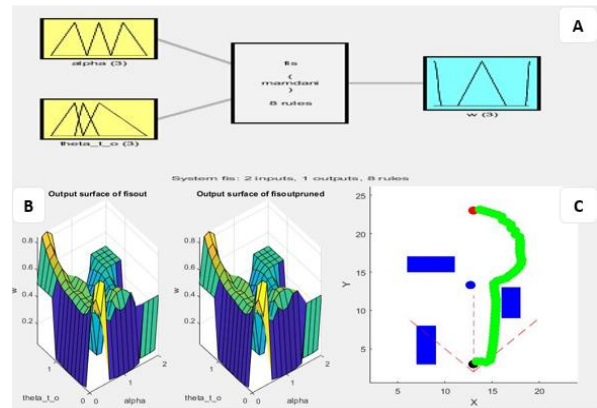


Figure 12: The Result of the First Experiment Where: A (Fuzzy System Interface), B (Output Surface of FLC), and C (Simulation for Obstacle Avoidance).

```

1 "alpha==low & theta_t_o==low => w=Medium (1)"
2 "alpha==Medium & theta_t_o==high => w=Medium (1)"
3 "alpha==low => w=high (1)"
4 "alpha==Medium & theta_t_o==Medium => w=low (1)"
5 "alpha==high & theta_t_o==low => w=high (1)"
6 "alpha==low & theta_t_o==Medium => w=Medium (1)"
7 "alpha==Medium & theta_t_o==low => w=low (1)"
8 "theta_t_o==high => w=low (1)"
    
```

Figure 13: Created Rules for the First Experiment by GA.

```

Angle
-----
-0.7854
-0.7854
-0.7854
-0.59632
0.00018724
0.00016968
0.0001545
    
```

Figure 14: Angles Created for the First Experiment by GA.

B. Test 2 (FLC+GA+2 Inputs and 4 MS)

In the second experiment, in Table 3, there are two inputs: alpha and theta. With four memberships function., and in Table 4 one output: weight with three memberships function.

Table 3: Membership Functions for Input Variable 'alpha and 'theta_t_o'.

Variable	Membership Function	Parameters
alpha	low	[0, 0.25, 0.5]
alpha	low_Medium	[0.5, 0.75, 1]
alpha	high_Medium	[1, 1.25, 1.5]
alpha	high	[1.5, 1.75, 2]
theta_t_o	low	[0, pi/10, pi/8]
theta_t_o	low_Medium	[pi/8, pi/7, pi/6]
theta_t_o	high_Medium	[pi/6, pi/5, pi/4]
theta_t_o	high	[pi/4, pi/2.75, pi/2]

Table 4: Membership Functions for Output Variable 'w'

Variable	Membership Function	Parameters
w	low	[0, 0.25]
w	Medium	[0.25, 0.5, 0.75]
w	high	[0.75, 1]

See Figure 15 shown below A, B, and C for the results of the second experiment. where the number of 16 rules were created after removing the unimportant rules that affect the accuracy of the robot's movement after evaluating the result. We also notice the effect of the GA on the creation of fuzzy rules and angles in Figure 16,17.

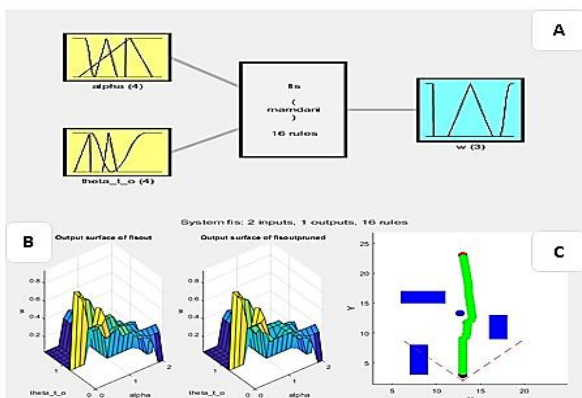


Figure 15: The Results of the Second Experiment were: A (Fuzzy System), B (Output Surface of FLC), and C (Simulation for Obstacle Avoidance).

```

1 "alpha==high_M & theta_t_o==low_M => w=low (1)"
2 "alpha==high & theta_t_o==high_M => w=low (1)"
3 "alpha==low_M & theta_t_o==high_M => w=low (1)"
4 "alpha==low_M & theta_t_o==high => w=low (1)"
5 "alpha==high & theta_t_o==high => w=low (1)"
6 "alpha==high_M & theta_t_o==low => w=M (1)"
7 "alpha==low & theta_t_o==low_M => w=M (1)"
8 "alpha==high & theta_t_o==low => w=low (1)"
9 "alpha==low_M => w=M (1)"
10 "alpha==low & theta_t_o==low => w=high (1)"
11 "alpha==low_M & theta_t_o==high_M => w=high (1)"
12 "theta_t_o==high => w=low (1)"
13 "alpha==low_M & theta_t_o==low_M => w=low (1)"
14 "alpha==high_M & theta_t_o==high_M => w=low (1)"
15 "theta_t_o==low_M => w=M (1)"
16 "alpha==low_M & theta_t_o==low => w=high (1)"
    
```

Figure 16: Created Rules for the Second Experiment by GA.



Figure 17: Angles Created for the Second Experiment by GA.

C. Test 3 (FLC+GA+2 Inputs and 6 MS)

In the third experiment, in Table 5, there are two inputs: alpha and theta. With six memberships function., and in Table 6 one output: weight with three memberships function.

Table 5: Membership Functions for Input Variable 'alpha and 'theta_t_o'

Variable	Membership Function	Parameters
alpha	lower	[0, 0.25, 0.5]
alpha	low	[0.25, 0.5, 0.75]
alpha	low_Medium	[0.5, 0.75, 1]
alpha	high_Medium	[0.75, 1, 1.5]
alpha	high	[1, 1.5, 1.75]
alpha	higher	[1.5, 1.75, 2]
theta_t_o	lower	[0, pi/10, pi/8]
theta_t_o	low	[pi/10, pi/8, pi/7]
theta_t_o	low_Medium	[pi/8, pi/7, pi/6]
theta_t_o	high_Medium	[pi/7, pi/6, pi/5]
theta_t_o	high	[pi/6, pi/5, pi/4]
theta_t_o	higher	[pi/5, pi/4, pi/2]

Table 6: Membership Functions for Output Variable 'w'

Variable	Membership Function	Parameters
w	low	[0, 0.25]
w	Medium	[0.25, 0.5, 0.75]
w	high	[0.75, 1]

We see in Figure 18 shows A, B, and C the result of the second experiment. where the number of 32 rules were created after removing the unimportant rules that affect the accuracy of the robot's movement after evaluating the result. We also notice the effect of the GA on the creation of the fuzzy rules and angles in Figure 19,20.

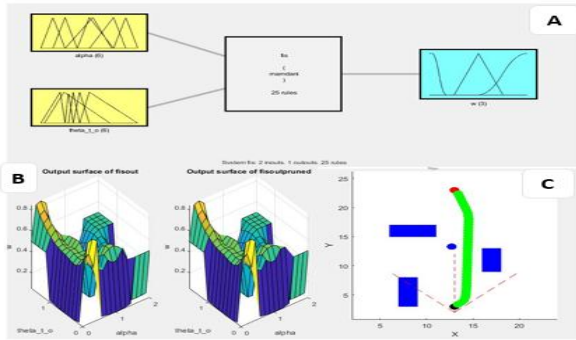


Figure 18: The Result of The Third Experiment where: A (fuzzy system), B (Output Surface of FLC), and C (Simulation for Obstacle Avoidance).

```

1 "alpha==high & theta_t_o==lower => w=low (1)"
2 "alpha==high_Medium & theta_t_o==lower => w=high (1)"
3 "theta_t_o==low => w=low (1)"
4 "alpha==lower & theta_t_o==low_Medium => w=low (1)"
5 "alpha==high_Medium & theta_t_o==low_Medium => w=high (1)"
6 "alpha==low_Medium => w=low (1)"
7 "alpha==low & theta_t_o==high_Medium => w=Medium (1)"
8 "alpha==low & theta_t_o==lower => w=low (1)"
9 "alpha==low_Medium & theta_t_o==high_Medium => w=Medium (1)"
10 "alpha==high & theta_t_o==higher => w=Medium (1)"
11 "alpha==high_Medium & theta_t_o==low => w=low (1)"
12 "alpha==low & theta_t_o==low => w=high (1)"
13 "alpha==low_Medium & theta_t_o==low_Medium => w=Medium (1)"
14 "alpha==lower & theta_t_o==low => w=Medium (1)"
15 "alpha==high & theta_t_o==high => w=Medium (1)"
16 "alpha==low_Medium & theta_t_o==lower => w=low (1)"
17 "alpha==higher & theta_t_o==lower => w=low (1)"
18 "alpha==higher & theta_t_o==high => w=Medium (1)"
19 "alpha==lower & theta_t_o==high_Medium => w=low (1)"
20 "alpha==lower & theta_t_o==lower => w=Medium (1)"
21 "alpha==lower => w=high (1)"
22 "alpha==low_Medium & theta_t_o==higher => w=low (1)"
23 "alpha==high & theta_t_o==low => w=low (1)"
24 "alpha==lower & theta_t_o==high => w=low (1)"
25 "alpha==lower & theta_t_o==higher => w=low (1)"
    
```

Figure 19: Created Rules for The Third Experiment by GA.

```

Angle
-0.78854
-0.78854
0.78854
0.36569
0.099402
0.054956
0.07769
0.000629
0.058884
0.014917
-0.0043751
-0.019733
-0.033751
-0.045446
-0.013999
-0.022451
0.20424
0.16756
0
    
```

Figure 20: Angles Created for The Third Experiment by GA.

Figures 12-C, 15-C, and 18-C illustrate the result of the simulation for obstacle collision avoidance, where the black circle indicates the starting point, the red circle indicates the destination, and the blue color indicates obstacles, the robot moves to a destination through the path line avoiding obstacles, and reach its destination with less time and shortest distance, and best deviation angle. it is observed in the three experiments that when the number of rules FLC in three experiments the accuracy of movement of the mobile robot increases, as he can choose the appropriate angles to avoid the obstacle with the lowest rate of deviation, and the shortest distance, to reach the desired destination in the shortest possible time and without distraction, shown in the Figures 13,14,16,17,19,20 the creation of fuzzy rules and the best deviation angles in the three experiments by GA. Figure 21 illustrates the best fitness values and mean fitness that appear on the comments window in MATLAB of three experiments of simulation collision avoidance of obstacles.

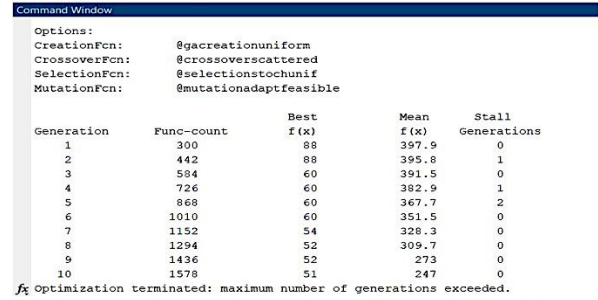


Figure 21: The Best Fitness Values and Mean Fitness of Three Experiments of Simulation Collision Avoidance of Obstacles.

Finally; Verify the tuned FLC's performance using various obstacles, and target positions, and use the tuned FIS to successfully avoid the obstacle and achieve the distraction position in the three experiment instances.

V. PROPOSED STUDY VS. RELATED STUDY

Show Table 7 comparison between the proposed study and related study.

Table 7: Proposed Study vs. Related Study

Study	The Proposed study	The study (W.Elmannai,2018)
Obstacle Detection Accuracy	Using CNN 99.9%	Using RGB-D 100%
Tracking Moving Obstacles	ROI with Kalman Filter to Track Moving Obstacles	----
Distance Measurement	Computer Vision 40meter	Computer Vision 9meter
Camera Stream	30Fps	30Fps
Average Number of Frames per Video	Varies by Video Time	700
Test Number	Recorded Video / 5	Real Video / 30
Guidance Movement	FLC	FLC
Optimization	GA	---

VI. CONCLUSION

The obstacle avoidance and safe guidance system based on three artificial intelligence technologies offers a promising solution to enhance the mobility and independence of blind individuals. by taking advantage of advanced technologies, such as deep learning, FLC decisions, and optimization using GA, the system provides obstacle detection using a CNN model that has been trained and reached an accuracy rate of 99.9% when tested. The system also tracks moving obstacles and measures the distance using methods of computer vision provides navigation assistance by providing movement guidance using three ultrasonic sensors, routing decisions using FLC, and improving system performance using GA to automatically generate fuzzy rule base and membership functions, allowing individuals using the system to navigate. safely and

confidently in different environments, this was shown through the experimental study conducted on the system to avoid collisions with obstacles. The study contributed

to the development of a collision avoidance system to help blind individuals by building an integrated intelligent hybrid system that integrates three artificial intelligence technologies (CNN, FLC, and GA), thus; the study contributed to improving these systems to help this category of society by using the sense of hearing as an alternative to the sense of vision. The study also recommends using a machine learning algorithm based on prediction to detect obstacles to reduce the risk of colliding with them.

REFERENCES

- [1] World Health Organization. *Visual Impairment and Blindness*. Accessed: Jun. 2023. [Online]. Available: <http://www.who.int/media-center/factsheets/fs282/en/>.
- [2] *Health Topics / Eye Care, Vision Impairment and Blindness*. Accessed: Jan. 2023. [Online]. Available: https://www.who.int/health-topics/blindness-and-vision-loss#tab=tab_1.
- [3] American Foundation for the Blind. Accessed: Jan. 2017. [Online]. Available: <http://www.afb.org/>
- [4] R. Velázquez, "Wearable assistive devices for the blind," in *Wearable and Autonomous Biomedical Devices and Systems for Smart Environment*, vol. 75. Berlin, Germany: Springer, Oct. 2010, pp. 331–349.
- [5] B. Douglas, "Wayfinding technology: A road map to the future," *J. Vis. Impairment Blindness*, vol. 97, no. 10, pp. 612–620, Oct. 2003.
- [6] B. B. Blasch, W. R. Wiener, and R. L. Welsh, *Foundations of Orientation and Mobility*, 2nd ed. New York, NY, USA: AFB Press, 1997.
- [7] C. Shah, M. Bouzit, M. Youssef, and L. Vasquez, "Evaluation of RU-Netra—Tactile feedback navigation system for the visually impaired," in *Proc. IEEE Int. Workshop Virtual Rehabil.*, Aug. 2006,
- [8] C. Shah and M. Bouzit, "Tactile feedback navigation handle for the Visually Impaired", p.117,2004.
- [9] W. Elmannai and K. Elleithy, "Sensor-based assistive devices for visually-impaired people: Current status, challenges, and future directions," *Sensors*, vol. 17, no. 3, p. 565, 2017.
- [10] H. Marion and A. J. Michael, "Assistive Technology for Visually Impaired and Blind People". London, U.K.: Springer, 2008.
- [11] V. Tiponut, D. Ianchis, M. E. Basch, and Z. Haraszky, "Work directions and new results in electronic travel aids for blind and visually impaired people", *WSEAS Trans. Syst.*, vol. 9, no. 10, pp. 1086–1097, 2011.
- [12] V. Tiponut, S. Popescu, I. Bogdanov, and C. Căleanu, "Obstacles detection system for visually-impaired guidance", in *Proc. New Aspects Syst. 12th WSEAS Int. Conf. Syst.*, Heraklion, Greece, Jul. 2008, pp. 350–356.
- [13] M. A. Hersh, "The design and evaluation of assistive technology products and devices part 1: Design," in *International Encyclopedia of Rehabilitation*. Buffalo, NY, USA: CIRRIE, 2010.
- [14] K. K. Kim, S. H. Han, J. Park, and J. Park, "The interaction experiences of visually impaired people with assistive technology: A case study of smartphones", *Int. J. Ind. Ergonom.*, vol. 55, pp. 22–33, Sep. 2016.
- [15] D. Dakopoulos and N. G. Bourbakis, "Wearable obstacle avoidance electronic travel aids for the blind: A survey", *IEEE Trans. Syst., Man, Cybern. C, Appl. Rev.*, vol. 40, no. 1, pp. 25–35, Jan. 2010.
- [16] L. Renier and A. G. De Volder, "Vision substitution and depth perception: Early blind subjects experience visual perspective through their ears", *Disab. Rehabil. Assistive Technol.*, vol. 5, no. 3, pp. 175–183, May 2010.
- [17] R. Tapu, B. Mocanu, and E. Tapu, "A survey on wearable devices used to assist the visually impaired user navigation in outdoor environments", in *Proc. IEEE 11th Int. Symp. (ISETC)*, Timișoara, Romania, Nov. 2014,
- [18] U. Yolo and Z. Xie, "A Multi-Sensory Guidance System for the Visually Impaired using Yolo and ORB-SLAM", pp. 1–17, 2022.
- [19] J. Liu, J. Liu, L. Xu, and W. Jin, "Electronic travel aids for the blind based on sensory substitution," in *Proc. 5th Int. Conf. Comput. Sci. Edu. (ICCSE)*, Hefei, China, Aug. 2010, pp. 1328–1331.
- [20] J. Sánchez and M. Elías, "Guidelines for designing mobility and orientation software for blind children," in *Human-Computer Interaction—INTERACT (Lecture Notes in Computer Science)*, vol. 14, C. Baranauskas, Eds. Rio de Janeiro, Brazil: Springer, Sep. 2007, pp. 375–388.
- [21] A. Dernayka, M. Amorim, R. Leroux, and A. Zogaghi, "Etude préliminaire d'un test de mesure de la capacité d'une personne à franchir un passage sans perception visuelle", November, 2022.
- [22] A. Zogaghi and R. Leroux, "Electronic travel aids and electronic orientation aids for blind people: Technical, rehabilitation and everyday life points of view," in *Proc. Conf. Workshop Assistive Technol. People Vis. Hearing Impairments Technol. Inclusion*, vol. 12. Nov. 2006, pp. 1–12.
- [23] S. Kammoun, M.-J. Macé, B. Oriola, and C. Jouffrais, "Toward a better guidance in wearable electronic orientation aids," in *Proc. IFIP Conf. Hum.-Comput. Interact.*, Lisbon, Portugal, Sep. 2011, pp. 624–627.
- [24] M. H. A. Wahab et al., "Smart cane: Assistive cane for visually-impaired people," *Int. J. Comput. Sci. Issues*, vol. 8, no. 4, pp. 21–27, Jul. 2011.
- [25] S. Bharambe, R. Thakker, H. Patil, and K. M. Bhurchandi, "Substitute eyes for blind with navigator using Android," in *Proc. India Edu. Conf. (TIIEC)*, Bengaluru, India, Apr. 2013, pp. 38–43.
- [26] Y. Yi and L. Dong, "A design of blind-guide crutch based on multi-sensors," in *Proc. IEEE 12th Int. Conf. Fuzzy Syst. Knowl. Discovery (FSKD)*, Zhangjiajie, China, Aug. 2015, pp. 2288–2292.
- [27] R. García, R. Fonseca, and A. Durán, "Electronic long cane for locomotion improving on visually impaired people. A case study," in *Proc. Pan Amer. Health Care Exchanges (PAHCE)*, Rio de Janeiro, Brazil, Mar./Apr. 2011, pp. 58–61.
- [28] J. J. M. Benjamin, Jr., "The laser cane," *Bull. Prosthetics Res*, pp. 443–50, 1974, [Online]. Available: <http://www.ncbi.nlm.nih.gov/pubmed/4462934>
- [29] K. Potdar, C. D. Pai, and S. Akolkar, "A Convolutional Neural Network based Live Object Recognition System as Blind Aid", 2018, [Online]. Available: <http://arxiv.org/abs/1811.10399>.
- [30] H. Son, D. Krishnagiri, V. S. Jeganathan, and J. Weiland, "Crosswalk Guidance System for the Blind", *Proc. Annu. Int. Conf. IEEE Eng. Med. Biol. Soc. EMBS*, vol. 2020-July, no. July, pp. 3327–3330, 2020, doi: 10.1109/EMBC44109.2020.9176623.
- [31] P. Alizadeh, "Object Distance Measurement Using a

- Single Camera for Robotic", p. 126, 2015.
- [33] [https:// www.roboflow.com/computer-vision-measure-distance/](https://www.roboflow.com/computer-vision-measure-distance/) 28 March 2023, Wednesday 05:00 AM.
- [34] <https://github.com/paul-pias/Object-Detection-and-Distance-Measurement> 28 March 2023, Wednesday 05:00 AM.
- [35] M. S. Farooq et al., "IoT Enabled Intelligent Stick for Visually Impaired People for Obstacle Recognition," *Sensors*, vol. 22, no. 22, pp. 1–20, 2022, doi: 10.3390/s22228914.
- [36] K. Kumar, B. Champaty, K. Uvanesh, R. Chachan, K. Pal, and A. Anis, "Development of an ultrasonic cane as a navigation aid for the blind people," in *Proc. Int. Conf. Control, Instrum., Commun. Comput. Technol. (ICCCCT)*, Kanyakumari, India, Jul. 2014, pp. 475–479.
- [37] S. Aymaz and T. Çavdar, "Ultrasonic assistive headset for visually impaired people", in *Proc. IEEE 39th Int. Conf. Jun. 2016*, pp. 388–391.
- [38] H. Batti, C. Ben Jabeur, and H. Seddik, "Mobile Robot Obstacle Avoidance in Labyrinth Environment Using Fuzzy Logic Approach", 2019, *Int. Conf. Control*.
- [39] C. Chen, H. Liu, H. Xiang, M. Li, Q. Pei, and S. Wang, "A rear-end collision avoidance scheme for intelligent transportation system", *MATEC Web Conf.*, vol. 81, pp. 1–6, 2016.
- [40] H. X. Zhang, B. Zhang, and F. Wang, "Automatic fuzzy rules generation using fuzzy genetic algorithm," *6th Int. Conf. Fuzzy Syst. Knowl. Discov. FSKD 2009*, vol. 6, pp. 107–112, 2009.
- [41] S., T. Kazadi," Conjugate schema and basis representation of crossover and mutation operators, *Evolution Computation*", vol. 6, pp.129-160, 1998.
- [42] G Syswerda," Uniform crossover in genetic algorithms", in *Proc. Of the Third Int. Conf on Genetic Algorithms*, 1989.
- [43] A. Tuson and P. Ross, *Adapting operator settings in genetic algorithms*, *Evolution Computation*, vol. 6, pp.161-184, 1998.
- [44] A. S. Wu and W. Banzhaf, "Introduction to the special issue: Variable-length representation and noncoding segments for evolutionary algorithms, *Evolution Computation*, vol. 6 pp.ii-vfi. 1998.
- [45] Yo-Ping Huang and Yueh-Tsun Chang, *Using Fuzzy Adaptive Genetic Algorithm for Function Optimization*, *IEEE*, pp 432-437, 2006
- [46] Wang Ke-jun.A new fuzzy genetic algorithm based on population diversity[C].*Proceedings of 2001 IEEE International Symposium on Computational Intelligence in Robots and Automation*, 2001:108-112.
- [47] M. Abdullah, "Mobile Robot Navigation using Potential Fields and market-based optimization," 2013.
- [48] Q. Liang, H. Zhou, W. Xiong, and L. Zhou, "Improved artificial potential field method for UAV path planning," *Proc. - 2022 14th Int. Conf. Meas. Technol. Mechatronics Autom. ICMTMA 2022*, vol. 2020, pp. 657–660, 2022, doi: 10.1109/ICMTMA54903.2022.00136.
- [49] <http://www.mathworks.com/help/fuzzy/tune-fuzzy-system-using-custom-cost-function.html> 3/December 2023, Sunday 02:00 AM.
- [50] S. Deshpande, A. K. Kashyap, and B. K. Patel, "A review on path planning AI techniques for mobile robots," *Robot. Syst. Appl.*, vol. 3, no. 1, pp. 27–46, 2023, doi: 10.21595/rsa.2023.23090.
- [51] W. M. Elmannai and K. M. Elleithy, "A novel obstacle avoidance system for guiding the visually impaired through the use of fuzzy control logic," *CCNC 2018 - 2018 15th IEEE Annu. Consum. Commun. Netw. Conf.*, vol. 2018-Janua, no. May, pp. 1–9, 2018.